

Chiral phosphinoferrocene carboxamides with amino acid substituents as ligands for Pd-catalysed asymmetric allylic substitutions. Synthesis and structural characterisation of catalytically relevant Pd complexes†

Jiří Tauchman, Ivana Císařová and Petr Štěpnička*

Received 28th June 2011, Accepted 16th August 2011

DOI: 10.1039/c1dt11230a

An extensive series of chiral amino acid amides prepared from 1'-(diphenylphosphino)ferrocene-1-carboxylic acid (Hd₂pf) or its planar-chiral isomer, 2-(diphenylphosphino)ferrocene-1-carboxylic acid, have been tested as ligands for Pd-catalysed asymmetric allylic substitution reactions. In alkylation of 1,3-diphenylallyl acetate as a model substrate with dimethyl malonate the ligands performed well in terms of both reaction rate and enantioselectivity, achieving up to 98% ee. In contrast, the reactions of the same substrate with other nucleophiles proceeded either slowly and with poor ee's (amination with benzylamine) or not at all (etherification with benzyl alcohol). In order to rationalise the influence of the ligand structure on the reaction course, three model complexes, *viz.* [(η³-methallyl)PdCl(L-κP)], [(η³-methallyl)Pd(L-κ²O,P)]ClO₄ and [(η³-methallyl)Pd(L-κP)₂]ClO₄ have been prepared from the achiral amide Ph₂PfcCONHCH₂CO₂Me (L; fc = ferrocene-1,1'-diyl) and structurally characterised. The coordination study showed that the amido-phosphines readily form 1 : 1 complexes as O,P-chelates where the amino acid chirality is brought close to the Pd atom. At higher ligand-to-metal ratios, however, simple P-monodentate coordination prevails, minimising the influence of the chiral amino acid pendant.

Introduction

Palladium-catalysed asymmetric allylic substitution is a powerful synthetic tool allowing for stereoselective construction of C–C and C–heteroatom bonds from a range of substrates.¹ Functional group tolerance and wide applicability in the synthesis of various chiral molecules led to a search for efficient ligands for this reaction, which meanwhile turned into a benchmark test for chiral donors. Particularly attractive proved to be donor-unsymmetric bidentate, potentially chelating ligands which electronically differentiate allylic termini in (η³-allyl)palladium intermediates and thus provide the necessary bias for the reaction to proceed selectively.^{1,2}

During the last few decades, numerous chiral, ferrocene-based donors of this kind have been developed and tested in allylic substitutions. As illustrious examples^{1g–h,3} may serve ferrocene diphosphines and the related mixed-donor ligands (mostly P,N- and P,O-donors), 2-ferrocenyl-4,5-dihydrooxazoles (oxazolines) and diphosphine diamides analogous to Trost's ligands.^{1,4}

In our previous work, we focused on catalytic utilisation of phosphinoferrocene carboxamides in Suzuki–Miyaura and Heck reactions⁵ and in asymmetric allylic alkylation.⁶ The favourable

catalytic properties and easy synthesis led us to extend our studies towards amides prepared from ferrocene phosphinocarboxylic acids and *amino acid* esters as a readily available chiral pool.⁷ Although similar ligands with organic backbones are known,⁸ this concept did not yet pervade the chemistry of ferrocene ligands.

This contribution details catalytic results obtained with a series of chiral phosphinoferrocene carboxamides bearing amino acid pendants (Scheme 1) in Pd-catalysed asymmetric allylic substitution reactions. Also reported are the preparation and structural characterisation of several (η³-allyl)Pd(II) complexes as models for the plausible reaction intermediates.

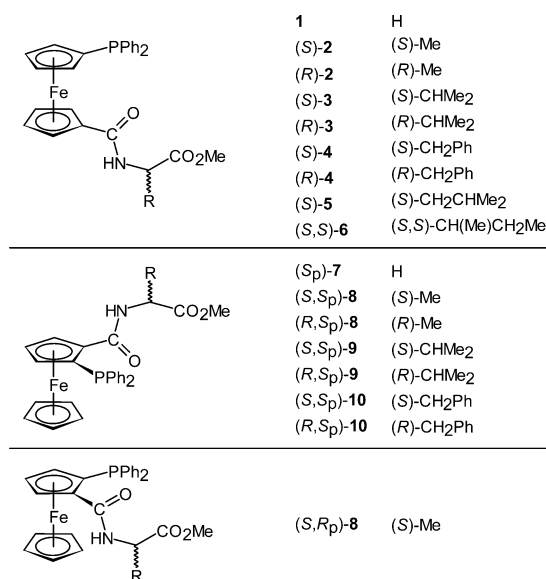
Results

The preparation of amino acid amides **1–4** and **7–10** was reported elsewhere.⁷ Two new ligands included in this study, (*S*)-**5** and (*S,S*)-**6**, were obtained in an analogous manner by amide coupling of 1'-(diphenylphosphino)ferrocene-1-carboxylic acid (Hd₂pf) with amino acid methyl esters formed *in situ* from the respective hydrochlorides and triethylamine.

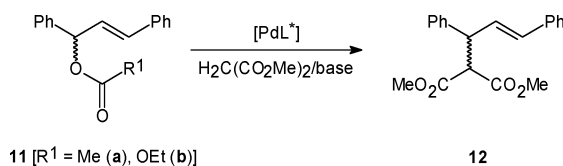
Chiral phosphine-amide ligands **2–10** (Scheme 1) were tested in palladium-catalysed asymmetric allylic alkylation using the common model reaction system comprising 1,3-diphenylallyl acetate (**11a**) as the allylic substrate and an 'instant' nucleophile⁹ generated from dimethyl malonate and *N,O*-bis(trimethylsilyl)-acetamide (BSA; Scheme 2). The pre-catalyst was formed

Department of Inorganic Chemistry, Faculty of Science, Charles University in Prague, Hlavova 2030, 12840, Prague, Czech Republic. E-mail: stepnic@natur.cuni.cz

† CCDC reference numbers 823874–823876. For crystallographic data in CIF or other electronic format see DOI: 10.1039/c1dt11230a



Scheme 1 Chiral phosphine-amide ligands tested in this study.



Scheme 2

in situ from $[\text{Pd}(\mu\text{-Cl})(\eta^3\text{-C}_3\text{H}_5)]_2$ and the respective ligand. Initial catalytic tests were carried out with ligands (S_p)-7 and (S)-2 as the representatives (Table 1).

The first catalytic tests with the planar-chiral ligand (S_p)-7 (Table 1, entries 1–8) already showed that the reaction proceeds with reasonable conversions and good ee's. Subsequent attempts to improve the reaction outcome by addition of catalytic amounts of alkali metal acetates (10% with respect to the allylic substrate) failed, the addition resulting in lower conversions and ee's. In contrast, cooling the reaction system containing only BSA to 0 °C considerably increased the enantioselectivity (ee 98%), albeit on account of the reaction rate (10% conversion after 24 h; entry 7). Addition of NaOAc as a base additive slightly improved the conversion at 0 °C but the ee dramatically decreased (entry 8).

A similar reaction with catalyst based on ligand (S)-2 featuring chirality only in the amino acid side chain was faster, affording complete conversion within 24 h (entries 9–16 in Table 1). Notably, however, the catalyst based on (S)-2 produced the alkylation product with the same degree of asymmetric induction as for (S_p)-7 but with an inverted ratio of the enantiomers ((S)-12 dominant; *cf.* entries 1 and 9). Similarly to (S_p)-7, the addition of alkali metal acetates to (S)-2/Pd system did not improve the catalytic performance, resulting in lower ee's while the conversions either remained virtually unchanged (Na and Cs) or decreased (Li, K and Rb). A decrease in the conversion and ee's was surprisingly noted also when the reaction temperature was lowered to 0 °C (entries 15 and 16).

Upon testing different solvents or bases (entries 17–27) it was found that the reaction becomes slower and less selective in THF and DMF, and stops entirely in dioxane or toluene. In acetonitrile,

Table 1 Summary of catalytic results obtained with ligands (S)-2 and (S_p)-7 in asymmetric allylic alkylation^a

Entry	Ligand	Solvent	Base/additive	Conv./%	ee/% [config] ^f
1	(S_p)-7	CH ₂ Cl ₂	BSA/none	81	85 [R]
2	(S_p)-7	CH ₂ Cl ₂	BSA/LiOAc	79	61 [R]
3	(S_p)-7	CH ₂ Cl ₂	BSA/NaOAc	80	81 [R]
4	(S_p)-7	CH ₂ Cl ₂	BSA/KOAc	54	55 [R]
5	(S_p)-7	CH ₂ Cl ₂	BSA/RbOAc	47	61 [R]
6	(S_p)-7	CH ₂ Cl ₂	BSA/CsOAc	75	64 [R]
7 ^b	(S_p)-7	CH ₂ Cl ₂	BSA/none	10	98 [R]
8 ^b	(S_p)-7	CH ₂ Cl ₂	BSA/NaOAc	24	37 [R]
9	(S)-2	CH ₂ Cl ₂	BSA/none	100	-85 [S]
10	(S)-2	CH ₂ Cl ₂	BSA/LiOAc	90	-67 [S]
11	(S)-2	CH ₂ Cl ₂	BSA/NaOAc	100	-65 [S]
12	(S)-2	CH ₂ Cl ₂	BSA/KOAc	80	-50 [S]
13	(S)-2	CH ₂ Cl ₂	BSA/RbOAc	84	-41 [S]
14	(S)-2	CH ₂ Cl ₂	BSA/CsOAc	100	-70 [S]
15 ^b	(S)-2	CH ₂ Cl ₂	BSA/none	10	-40 [S]
16 ^b	(S)-2	CH ₂ Cl ₂	BSA/NaOAc	90	-58 [S]
17	(S)-2	THF	BSA/none	56	-45 [S]
18	(S)-2	dioxane	BSA/none	0	—
19	(S)-2	toluene	BSA/none	0	—
20	(S)-2	MeCN	BSA/none	100	-77 [S]
21	(S)-2	DMF	BSA/none	67	-74 [S]
22	(S)-2	CH ₂ Cl ₂	NaN(SiMe ₃) ₂	49	-26 [S]
23	(S)-2	CH ₂ Cl ₂	KN(SiMe ₃) ₂	11	-20 [S]
24	(S)-2	CH ₂ Cl ₂	KO ^{<i>t</i>} -Bu	72	-4 [S]
25	(S)-2	CH ₂ Cl ₂	K ₂ CO ₃	5	—
26	(S)-2	CH ₂ Cl ₂	K ₃ PO ₄	37	0
27	(S)-2	CH ₂ Cl ₂	DBU ^c	82	-6 [S]
28 ^c	(S)-2	CH ₂ Cl ₂	BSA/none	0	—
29 ^c	(S)-2	CH ₂ Cl ₂	BSA/NaOAc	0	—
30 ^d	(S)-2	CH ₂ Cl ₂	BSA/none	100	-78 [S]
31 ^d	(S)-2	CH ₂ Cl ₂	BSA/NaOAc	100	-61 [S]

^a Reaction of **11a** with 3 equiv. of dimethyl malonate and 3 equiv. of BSA in the presence of 5 mol.% of Pd catalyst generated *in situ* from $[\text{Pd}(\mu\text{-Cl})(\eta^3\text{-C}_3\text{H}_5)]_2$ and a ligand (Pd:L = 1:1) in 3 mL of solvent at room temperature for 24 h. ^b Reaction performed at 0 °C. ^c Reaction with di-*tert*-butyl malonate. ^d Reaction with **11b** as the substrate. ^e DBU = 1,8-diazabicyclo[5.4.0]undec-7-ene. ^f ee = ($[R] - [S]$)/($[R] + [S]$).

the conversion remained high but selectivity decreased (conversion 100% after 24 h, ee = -77% with (S)-2). The use of bases other than BSA also resulted in lower conversions and markedly decreased the enantioselectivity. Finally, changing the reaction partners (entries 28–31) had a detrimental effect on the reaction outcome. The reaction with **11a** and di-*tert*-butyl malonate as a more bulky nucleophile did not proceed while carbonate **11b** and dimethyl malonate afforded the alkylation product still quantitatively but with a relatively lower selectivity.

Additional experiments with ligand (S)-2 revealed that the reaction outcome depends strongly on the ligand-to-metal ratio (results not tabulated). Whereas the conversions achieved with (S)-2 remained practically complete in all cases (98–100% after 24 h), the enantioselectivity decreased from ee -85% at L:Pd ratio 1:1 to -71% at L:Pd = 1:1.2 and -62% at L:Pd = 1:1.5 and, finally, to zero at L:Pd = 2:1. A similar but less pronounced trend was noted also in reactions with ligand (S_p)-7, which afforded the alkylation product with 81% conversion and 85% ee at L:Pd ratio 1:1 and with an 82% conversion and 77% ee at L:Pd ratio 2:1.

After surveying the reaction parameters, the whole series of ligands was assessed under optimised conditions (BSA without any added alkali metal acetate, dichloromethane, room temperature). The results are summarised in Table 2.

Table 2 Survey of the ligands in the Pd-catalysed allylic alkylation^a

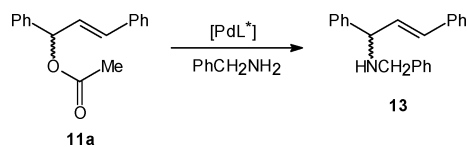
Amino acid	Hdpf		(S _p)-Hpfc	
	Ligand	Conv./% ee/%	Ligand	Conv./% ee/%
Gly	1	—	(S _p)- 7	81 [R] 85 [R]
(S)-Ala	(S)- 2	100 -85 [S]	(S,S _p)- 8	55 [R]
(R)-Ala	(R)- 2	100 84 [R]	(R,S _p)- 8^b	34 [R] 83 [R]
(S)-Val	(S)- 3	23 -24 [S]	(S,S _p)- 9	80 [R] 60 [R]
(R)-Val	(R)- 3	25 26 [R]	(R,S _p)- 9	12 [R] 57 [R]
(S)-Leu	(S)- 5	93 -65 [S]	—	—
(S,S)-Ile	(S,S)- 6	53 -11 [S]	—	—
(S)-Phe	(S)- 4	56 -67 [S]	(S,S _p)- 10	51 [R] 65 [R]
(R)-Phe	(R)- 4	92 66 [R]	(R,S _p)- 10	15 [R] 58 [R]

^a For conditions, see Table 1, footnote a. Data for compounds (S)-**2** and (S_p)-**7** are included from Table 1 for a comparison. ^b The enantiomeric ligand (S,R_p)-**8** gave **12** with 43% conversion and -85% ee.

In general, the reaction rate (conversion) and stereoselectivity varied greatly with the ligand structure. Reactions with ligands derived from achiral Hdpf and (S)-amino acid esters produced the alkylation product enriched in (S)-**12**, while the enantiomeric ligands expectedly favoured the formation of (R)-**12**. Among donors obtained from (S)-amino acids, which constitute a more extensive set, the best conversion and ee were achieved with (S)-**2** as a ligand possessing the smallest substituent in the amino acid residue. Increasing the steric bulk of the amino acid substituent significantly decreased the enantioselectivity. For instance, (S)-**5** featuring an amino acid residue branched in γ -position and the ligand obtained from (S)-phenylalanine afforded the alkylation product with a lower, *ca.* 65–67% ee. The more sterically encumbered ligands branched in β -position ((S)-**3** and (S,S)-**6**) performed even worse (Table 2).

Trends among ligands derived from planar-chiral 2-(diphenylphosphino)ferrocene-1-carboxylic acid (Hpfc) are less obvious, probably because of an interplay of the two chirality elements. Yet again, the best results were obtained with ligand (S_p)-**7** containing the least sterically demanding glycine pendant.

Ligand (S)-**2** was chosen for further testing in allylation of model N- and O-nucleophiles. Amination performed with **11a** and benzylamine in the presence of BSA as a base (Scheme 3, Table 3) afforded only racemic **13** (96% conversion after 2 days with 5% mol.% of Pd catalyst). Similar reactions without any additive proceeded much slower and with only a poor enantioselectivity (Table 3). An analogous etherification of **11a** with benzyl alcohol (Scheme 4) in the presence of 5 mol.% of the same Pd-catalyst and BSA or Cs₂CO₃ as the base (3 equiv.) did not proceed at all.

**Scheme 3**

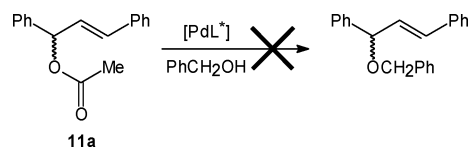
Coordination study

In order to gain an insight into the nature of putative reaction intermediates and structural factors governing the reaction course, we decided to synthesise and *structurally* characterise some model (η^3 -allyl)palladium(II) complexes. Unfortunately, repeated

Table 3 Summary of catalytic results obtained in allylic amination^a

Entry	Base	t/h	Conv. (ee)/%
1	BSA	24	62 (0)
2	BSA	48	96 (0)
3	none	24	20 (12) [R]
4	none	48	29 (13) [R]

^a Conditions: 5 mol.% Pd catalyst prepared *in situ* from [Pd(μ -Cl)(η^3 -C₃H₃)₂] and (S)-**2** (L : Pd = 1 : 1); PhCH₂NH₂ (3 equiv.), BSA (3 equiv.) in CH₂Cl₂ (3 mL), room temperature.

**Scheme 4**

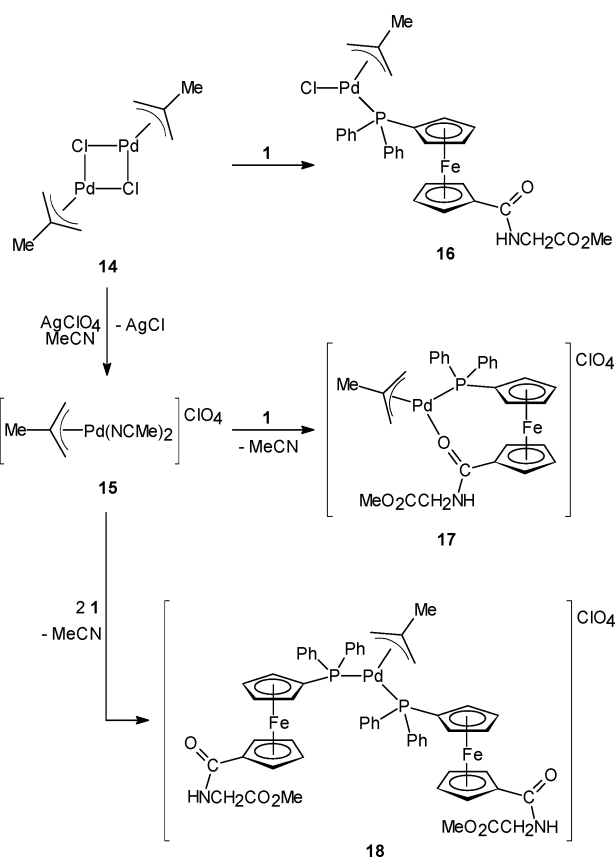
attempts to prepare any well-defined (solid) samples of the most catalytically relevant (η^3 -1,3-diphenylallyl)palladium complexes with (S)-**2** failed.¹⁰ Therefore, we turned to similar reactions with achiral donor **1**.¹¹

Indeed, the reaction of [(η^3 -Ph₂C₃H₃)PdCl]₂ and **1** produced an orange solid, which showed a signal due to [(η^3 -Ph₂C₃H₃)Pd(**1**)]⁺ (*m/z* 784) in ESI mass spectra and contained one dominant and two very minor species according to ¹H (ref.)¹² and ³¹P NMR analysis. The NMR spectra suggested that the PPh₂ group is coordinated in all cases (δ_p 14.8 major, 15.5 and 16.0 minor). Considering the high conformational flexibility of (η^3 -Ph₂C₃H₃)Pd moiety and similarity of the ³¹P NMR chemical shifts, the minor components are most probably isomers to the major component differing in the overall molecular conformation. However, other species resulting by, *e.g.*, self-ionisation ([(η^3 -Ph₂C₃H₃)PdCl(**1**)] → [(η^3 -Ph₂C₃H₃)Pd(**1**)]Cl), cannot simply be excluded.

When AgClO₄ (1 equiv.) was added to *in situ* formed [(η^3 -Ph₂C₃H₃)PdCl(**1**)], the chloride complex was cleanly converted to a new compound, which showed one broad, low-field shifted signal in its ³¹P NMR spectrum (δ_p 19.5). The ¹H NMR spectrum displayed *very* broad resonances, suggesting some dynamic equilibria. The ESI mass spectrum expectedly showed a peak at *m/z* 784 ([(η^3 -Ph₂C₃H₃)Pd(**1**)]⁺).

Because our subsequent attempts at obtaining crystalline materials from [(η^3 -Ph₂C₃H₃)PdCl(**1**)] and [(η^3 -Ph₂C₃H₃)Pd(**1**)]ClO₄ met with no success, we ultimately turned to η^3 -methallyl complexes with non-chiral ligand **1** as even simpler (an potentially better crystallising) compounds (Scheme 5). Thus, the dipalladium complex **14** reacted smoothly with **1** yielding the bridge-cleavage product **16** in which the ferrocene ligand coordinates as a P-monodentate donor. The reactions of **1** with complex **15**, which was obtained from **14** *via* halogen abstraction with AgClO₄,¹³ proceeded under displacement of the coordinated acetonitrile ligands to afford complex **17** featuring the amidophosphine as an O,P-chelate donor or bis-phosphine complex **18** depending on the Pd/**1** molar ratio. According to NMR analysis of the reaction mixtures, the complexation reactions proceed cleanly, affording only the products specified.

Complexes **16** and **17** are highly soluble in common organic solvents and were therefore isolated by precipitation as yellow air-stable solids showing a high tendency to hold solvent residua. The



Scheme 5 Preparation of (η^3 -methylallyl)palladium complexes.

solubility of complex **18** is relatively lower. It is noteworthy that complex **16** did not appreciably react with BSA, $\text{NaN}(\text{SiMe}_3)_3$ or $\text{KO}t\text{-Bu}$ (2 equiv.; reactions in CH_2Cl_2 at room temperature for *ca.* 20 h). In contrast, addition of NaH and stirring overnight caused extensive decomposition.

Complexes **16–18** exhibit single resonances in their $^{31}\text{P}\{^1\text{H}\}$ NMR spectra, shifted markedly to lower fields *versus* free **1** due to P-coordination of the ferrocene ligand (*cf.* **16**: $\delta_{\text{P}} = 11.6$, **17**: $\delta_{\text{P}} = 20.8$, **18**: $\delta_{\text{P}} = 18.2$; **1**: $\delta_{\text{P}} = -16.9$). Coordination of the amide oxygen in **17** is manifested by a shift of the associated ^{13}C NMR resonance to lower fields (*cf.* $\delta_{\text{C}}(\text{CONH})$ *ca.* 170 for **16** and **18**, and *ca.* 174 for **17**) and further in IR spectra, where the amide I band (largely $\nu_{\text{C=O}}$) moves to lower energies (1652/1655 cm^{-1} for **16/18** *vs.* 1596 cm^{-1} for **17**) while the amide II band shifts in the opposite direction (1538/1536 cm^{-1} for **16/18** and 1558 cm^{-1} for **17**).^{6b,7a} The response of the terminal ester group, which is not involved in coordination, remains practically unaffected ($\nu_{\text{C=O}} \approx 1750 \text{ cm}^{-1}$, $\delta_{\text{C}} \approx 170$).

The non-equivalent allylic CH_2 groups in **16** and **17** give rise to two pairs of signals ($\text{H}^{\text{syn/anti}}$) in the ^1H NMR and two separate signals in the $^{13}\text{C}\{^1\text{H}\}$ NMR spectra. For both compounds, the low-field ^{13}C NMR signals show splitting with ^{31}P ($\delta_{\text{C}} 78.65$ for **16**, 83.34 for **17**; $^2J_{\text{PC}}$ *ca.* 30 Hz) and can thus be attributed to the CH_2 groups located *trans* to the phosphorus donor atom. The signals due to CH_2 *trans* to Cl or O appear as singlets at higher fields ($\delta_{\text{C}} 64.13$ for **16**, and 55.44 for **17**). It is noteworthy that a larger difference in the ^{13}C chemical shifts in this case corresponds to a larger difference in *trans*-influence of the respective donor groups ($\Delta_{\text{P/Cl}} < \Delta_{\text{P/O}}$) and also in the lengths of the $\text{Pd}-\text{CH}_2$ bonds (see below).

Allylic CH_2 groups in complex **18** are equivalent, being observed as a pair of signals in the ^1H NMR spectrum and one ^{13}C NMR resonance which overlaps with the solvent signal ($\delta_{\text{C}} \approx 76.6$). Owing to the presence of two identical phosphine groups in **18**, the $^{13}\text{C}\{^1\text{H}\}$ NMR signals due to carbons within the Ph_2P -substituted cyclopentadienyl and phenyl rings (except for CH_{para}) and signal of the allylic C_{ipso} carbon are seen as characteristic non-binomial triplets typical of virtually coupled ABX spin systems of the type $^{12}\text{C}-^{31}\text{P}(\text{A})-\text{M}-^{31}\text{P}(\text{B})-^{13}\text{C}(\text{X})$ ($\text{M} = \text{metal}$).¹⁴ Similar features were observed in the spectra of bis-phosphine complexes with other 1'-functionalised (diphenylphosphino)ferrocene ligands, *trans*- $[\text{PdCl}_2(\text{Ph}_2\text{PfcX-}\kappa\text{P})_2]$ ($\text{X} = \text{a functional group}$)¹⁵ and *trans*- $[\text{W}(\text{CO})_4(\text{Ph}_2\text{PfcCH}=\text{CH}_2-\kappa\text{P})_2]$.¹⁶

Crystal structures. Complex **15** (Fig. 1) crystallises in the monoclinic space group $\text{P}2_1/m$ so that both ions constituting the structure reside on the crystallographic mirror planes, similar to $[\text{Pd}(\eta^3\text{-C}_3\text{H}_5)(\text{MeCN})_2(\text{B}_{10}\text{H}_{10})\text{-C}_6\text{H}_6]$.¹⁷ Similarly to other π -allyl complexes,¹⁸ the allyl plane is tilted with respect to the plane defined by palladium and its ligating nitrogen atoms, $\{\text{Pd}, \text{N}, \text{N}'\}$, at the dihedral angle of $117.4(2)^\circ$. The $\text{Pd}-\text{C}_{\text{terminal}}$ distance in **15** is by *ca.* 0.04 Å shorter than the $\text{Pd}-\text{C}_{\text{meso}}$ bond and the methyl group in *meso* position is displaced from the allyl plane $\{\text{C}1, \text{C}2, \text{C}1'\}$ towards the Pd atom by 0.301(3) Å. The geometry of the $\text{Pd}-\text{NCMe}$ moiety in **15** compares well with that in the mentioned $\eta^3\text{-C}_3\text{H}_5$ complex. In the crystal, the ions constituting the structure of **15** are interconnected *via* $\text{C}-\text{H} \cdots \text{O}$ interactions¹⁹ into layers oriented parallel to the *ab* plane.

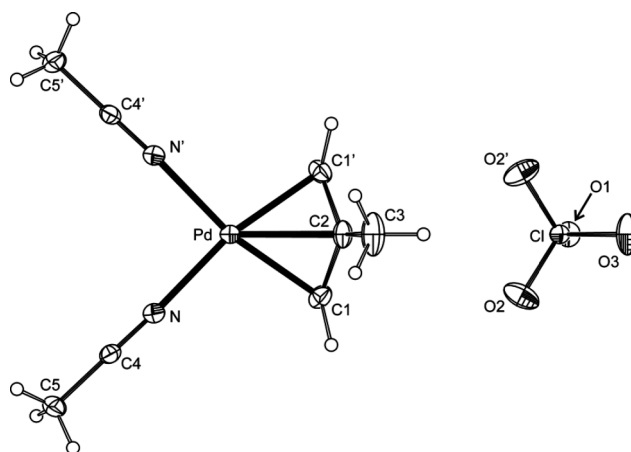


Fig. 1 PLATON plot of the molecular structure of **15** (30% probability level). Primed atoms are generated by the $(x, \frac{1}{2} - y, z)$ symmetry operation. Selected distances and angles (in Å and deg): $\text{Pd}-\text{N}$ 2.079(1), $\text{N}-\text{C}4$ 1.131(2), $\text{C}4-\text{C}5$ 1.454(2), $\text{Pd}-\text{N}-\text{C}4$ 176.8(1), $\text{N}-\text{C}4-\text{C}5$ 179.6(3); $\text{Pd}-\text{C}1$ 2.103(2), $\text{Pd}-\text{C}2$ 2.144(2), $\text{C}1-\text{C}2$ 1.402(2), $\text{C}2-\text{C}3$ 1.501(4), $\text{C}1-\text{C}2-\text{C}1'$ 114.7(2); $\text{Cl}-\text{O}$ 1.429(2)–1.439(2), $\text{O}-\text{Cl}-\text{O}$ 109.03(9)–109.8(1).

The molecular structures of **16**- H_2O and **17** are presented in Fig. 2 and 3. Selected distances and angles are given in Table 4. The Pd-donor (Cl, O, P, and allyl carbons) distances in **16**- H_2O and **17** are unexceptional in view of the data reported for $[(\eta^3\text{-methylallyl})\text{PdCl}(\text{L}-\kappa\text{P})]$ ($\text{L} = \text{PPh}_3$ ²⁰ or Hdpp ²¹) and the O,P-chelate complexes $[(\mu\text{-O,P:O',P'-L}^1)\text{Pd}_2(\eta^3\text{-C}_3\text{H}_5)_2](\text{OTf})_2$ ($\text{L}^1 = (R,R)\text{-1,2-(2-Ph}_2\text{PC}_6\text{H}_4\text{CONH)C}_6\text{H}_{10}$; Trost's ligand)²² and $[\text{Pd}(\eta^3\text{-1,3-Ph}_2\text{C}_3\text{H}_5)(\text{L}^2-\kappa^2\text{O,P})]$ ($\text{L}^2 = [\text{Fe}(\eta^5\text{-C}_5\text{H}_5\text{-1-PPh}_2\text{-2-CONHCH}_2\text{Ph})(\eta^5\text{-C}_5\text{H}_5)]$).^{6b} The allyl unit in **16**- H_2O extends away from the

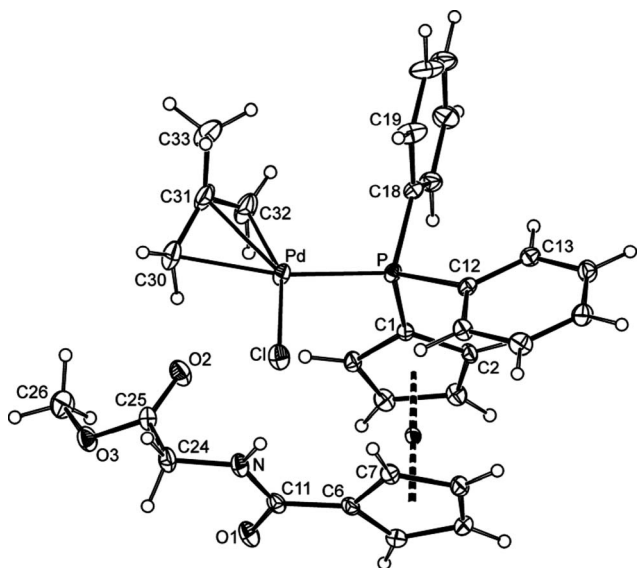


Fig. 2 PLATON plot of the complex molecule (major contributing part) in $16 \cdot \text{H}_2\text{O}$. Displacement ellipsoids enclose the 30% probability level.

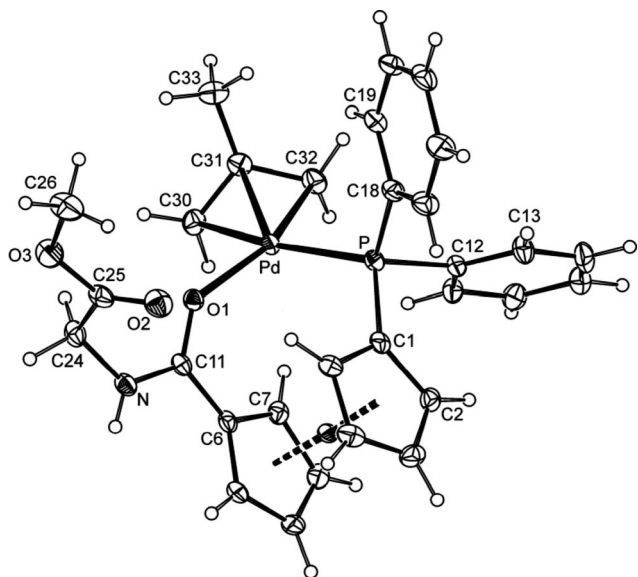


Fig. 3 PLATON plot of the complex cation the crystal structure of 17 . Displacement ellipsoids enclose the 30% probability level.

ferrocene unit and above the amino acid residue whereas in 17 it is embedded within a donor pocket created by the chelate ligand.²³ The allyl planes are tilted with respect to the plane defined by the Pd and the σ -donor atoms (the dihedral angles are $115.5(3)^\circ$ for $16 \cdot \text{H}_2\text{O}$ and $112.1(5)^\circ$ for 17) and the methyl substituent is inclined towards palladium (the distances of the methyl carbon from the allyl planes are $0.271(5) \text{ \AA}$ for $16 \cdot \text{H}_2\text{O}$ and $0.248(6) \text{ \AA}$ for 17). In both structures, the Pd–C(allyl) bond lengths gradually decrease from C30 to C32. A smaller absolute difference in $16 \cdot \text{H}_2\text{O}$ (*cf.* *ca.* 0.09 \AA for $16 \cdot \text{H}_2\text{O}$ and *ca.* 0.12 \AA for 17) corresponds with the nature of donors in *trans* positions (*trans*-influence: $\text{PR}_3 > \text{Cl} > \text{O}$).²⁴ The allylic C–C bond lengths follow a similar though less pronounced trend.

Change in the mode of coordination such in $16 \cdot \text{H}_2\text{O}$ and 17 obviously alters the geometry of the ferrocene ligand. The

Table 4 Selected geometric data (in \AA and $^\circ$) for $16 \cdot \text{H}_2\text{O}$ and 17^a

Parameter	$16 \cdot \text{H}_2\text{O}$ (X = Cl) ^d	17 (X = O1)
Pd–X	2.3730(8)	2.142(3)
Pd–P	2.3163(7)	2.313(1)
Pd–C30	2.198(3)	2.210(5)
Pd–C31	2.173(3)	2.173(4)
Pd–C32	2.110(3)	2.087(4)
X–Pd–P	106.09(3)	101.76(8)
X–Pd–C30	93.35(9)	94.2(1)
P–Pd–C32	93.56(9)	97.4(1)
C30–Pd–C32	66.7(1)	67.0(2)
C30–C31	1.394(4)	1.388(6)
C31–C32	1.425(4)	1.428(6)
C31–C33	1.485(5)	1.497(6)
C30–C31–C32	114.4(3)	114.9(4)
C30/C32–C31–C33	122.0(3)/122.4(3)	122.3(4)/121.9(4)
C11–O1	1.235(3)	1.249(5)
C11–N	1.340(3)	1.326(4)
O1–C11–N	121.6(2)	120.1(3)
O1–C11–N–C24	0.5(4)	3.3(6)
φ^b	6.3(3)	21.8(5)
C25–O2	1.198(4)	1.190(6)
C25–O3	1.328(4)	1.335(5)
O2–C25–O3	124.8(3)	124.9(4)
Fe–Cg1	1.647(1)	1.645(2)
Fe–Cg2	1.650(1)	1.649(2)
$\angle \text{Cp1, Cp2}$	3.4(2)	5.9(3)
τ^c	85	63

^a Definition of the ring planes: Cp1 = C(1–5), Cp2 = C(6–10). Cg1/2 denote the respective ring centroids. ^b Dihedral angle subtended by the amide {C11, O1, N} and Cp2 ring planes. ^c Torsion angle C1–Cg1–Cg2–C6. ^d Data for the major contributing part (see Experimental).

closure of the O,P-chelate ring requires reorientation of the cyclopentadienyl (Cp) rings and rotation of the amide plane from an arrangement coplanar with its parent cyclopentadienyl ring. The amide moieties C(O)NHCH₂ in both structures are practically planar (see the O1–C11–N–C24 torsion angles in Table 4) but assume mutually opposite orientations. In $16 \cdot \text{H}_2\text{O}$, the amide plane is oriented with its N atom to the side of the phosphorus substituent while in 17 the amide oxygen is closer to PPh₂ due to chelation. Furthermore, the coordination results in a slight elongation of the C=O and shortening of the C–N amide bonds (uniformly by $\pm 0.014 \text{ \AA}$). Similar changes can be detected in the structures of the mentioned bis[(allyl)palladium] complex featuring Trost's ligand²² and in Pd(II) complexes with phosphinoferrrocene carboxamides.^{6b,7a}

It also is noteworthy that complex 16 isolated from the reaction mixture is amorphous and does not crystallise under anhydrous conditions. The crystallisation commences readily once some adventitious water is present, affording the stoichiometric solvate $16 \cdot \text{H}_2\text{O}$. The reason for such behaviour becomes evident upon inspection of the crystal assembly. The water molecules in $16 \cdot \text{H}_2\text{O}$ behave as molecular clips, connecting two adjacent molecules of the complex into a centrosymmetric array *via* hydrogen bonds to carbonyl oxygen as a bifurcate H-bond acceptor (Fig. 4). The amide NH group oriented towards the (allyl)Pd unit forms an intramolecular hydrogen bond with the Pd-bound chloride. On the other hand, the solid-state packing of non-solvated 17 is dominated by hydrogen bonds between NH²⁵ and CH protons as H-bond donors and perchlorate oxygen atoms as acceptors.

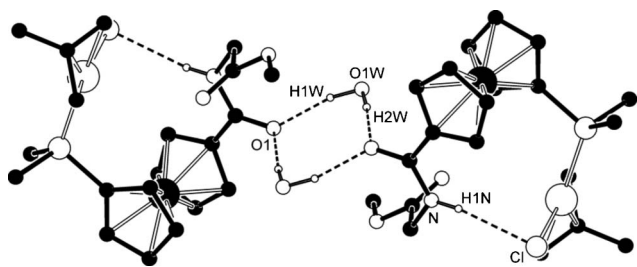


Fig. 4 Hydrogen bonding interactions (dashed lines) in the structure of **16**·H₂O. For clarity, only relevant hydrogen atoms and pivotal carbons of the phenyl rings are shown. H-bond parameters are as follows: O1W–H1W···O1, O1W···O1 = 2.863(3) Å, angle at H1W = 167°; O1W–H2W···O1, O1W···O1 = 2.895(3) Å, angle at H2W = 172°; N1–H1N···Cl, N1···Cl = 3.292(2) Å, angle at H1N = 158°.

Discussion and conclusion

Unlike many other chiral phosphinoferrrocene ligands obtained by multi-step procedures, the chiral amides prepared by conjugation of ferrocene phosphinocarboxylic acids with amino acid esters are readily accessible in good yields and purity and, above all, are highly structurally versatile. The results collected indicate that these amides are efficient ligands for Pd-catalysed asymmetric allylic alkylation. In the model reaction of dimethyl malonate with in the presence of BSA, they produce the alkylation product with up to 98% ee under optimised reaction conditions. On the other hand, the ligands perform only poorly in the corresponding amination and etherification reactions.

The model coordination study expectedly demonstrated that the phosphine-amide ligands coordinate the soft palladium(II) ion²⁶ preferentially *via* their soft P-donor site. At 1 : 1 metal-to-ligand ratio, however, they form chelates. Although this has not been proven *in situ* (*i.e.*, under conditions mimicking exactly the reaction mixture), the formation of chelated Pd(II) intermediates appears to be the only plausible explanation for the observed reaction outcome. Regardless of whether O,P- (neutral ligand) or P,N-chelates (deprotonated ligand) are formed as catalytically active intermediates, the chelation brings the chirality inherent in the amino acid into a vicinity of the catalytic centre. The catalysed reaction (conversion *and* ee) is then controlled largely by spatial properties of the amino acid substituent. Besides, the coordination of two different donor atoms leads to an electronic differentiation of allylic termini in (η^3 -allyl)palladium(II) reaction intermediates (see structural data above), which then react with relatively different rates with the incoming nucleophile (preferentially at the site opposite to the donor with a larger *trans*-influence).^{1,27}

Increasing the Pd-to-ligand ratio to 1 : 2 results in the formation of bis(phosphine) complexes, where the amino acid chirality is located rather far from the catalytic centre. This particularly holds true for ligands obtained from achiral Hdprf, with which only racemic alkylation product was obtained at the Pd:L ratio of 1 : 2.

The situation becomes more complicated (and less predictable) upon introduction of planar chirality into the system mostly because the chirality elements may combine in a matched or a mismatched manner (*cf.* the catalytic performance of (*S,S*_p)- and (*R,S*_p)-**8**). In addition, the donor groups attached in positions 1 and 2 of the ferrocene moiety are closer to each other than in

the Hdprf-based ligands, which may result in sterically crowded intermediates and a diminished preference for a single reaction intermediate.

Experimental

Materials and methods

All syntheses were performed under an argon atmosphere with exclusion of the direct daylight. Solvents used in the syntheses and catalytic tests were dried over by appropriate drying agents and distilled under argon: dichloromethane (K₂CO₃), 1,4-dioxane, toluene and tetrahydrofuran (sodium metal). Anhydrous acetonitrile and *N,N*-dimethylformamide were purchased from Fluka. Methanol was distilled from MeONa. Benzylamine and benzyl alcohol were distilled under vacuum. Amino acid methyl ester hydrochlorides [H₃NCH(R)CO₂Me]Cl (R = (*S*)-CH₂CHMe₂ and (*S,S*)-CHMeCH₂Me) were prepared by reactions of the respective amino acids with thionyl chloride in dry methanol.²⁸ Hdprf,²⁹ ligand **1**^a and its chiral analogues (**2–4**, **7–10**),^{7b} *rac*-1,3-diphenylprop-2-en-1-yl acetate (**11a**),³⁰ *rac*-ethyl-(1,3-diphenylprop-2-en-1-yl) carbonate (**11b**),³¹ *rac*-*N*-benzyl-(1,3-diphenylprop-2-en-1-yl)amine (**13**),³² and [Pd(μ -Cl)(η^3 -MeC₃H₄)₂] (**14**)³³ were prepared according to literature procedures. Other chemicals (Aldrich, Fluka) and solvents used for crystallisations and in chromatography (Lach-Ner) were used as received.

NMR spectra were recorded with a Varian UNITY Inova 400 spectrometer (¹H, 399.95 MHz, ¹³C, 100.58 MHz; and ³¹P, 161.90 MHz) at 298 K. Chemical shifts (δ (ppm)) are given relative to internal SiMe₄ (¹H and ¹³C) or to external 85% aqueous H₃PO₄ (³¹P). IR spectra were obtained with an FT IR Nicolet Magna 760 instrument. High resolution electrospray ionisation mass spectra (ESI MS) were obtained with an LTQ Orbitrap XL spectrometer (Thermo Fisher Scientific). Optical rotations were determined with an automatic polarimeter Autopol III (Rudolph Research) at room temperature.

Safety Note. Caution! Although we have not encountered any problems it should be noted that perchlorate salts of metal complexes with organic ligands are potentially explosive and should be handled only in small quantities and with care.

Syntheses and catalytic tests

N-[(1*S*)-1-methoxycarbonyl-3-methylbutyl] [1'-(diphenylphosphino)ferrocene-1-carboxamide] ((*S*)-**5**). Hdprf (207 mg, 0.50 mmol) and 1-hydroxybenzotriazole (81 mg, 0.60 mmol) were mixed with dry dichloromethane (10 mL). The suspension was cooled in an ice bath and treated with 1-(3-dimethylaminopropyl)-3-ethylcarbodiimide (0.1 mL, 0.6 mmol). The resultant mixture was stirred at 0 °C for 15 min, whereupon the solids dissolved to give a clear orange-red solution. A mixture of (*S*)-[H₃NCH(CH₂CHMe₂)CO₂Me]Cl (127 mg, 0.70 mmol), triethylamine (0.1 mL, 0.8 mmol) and dichloromethane (20 mL) prepared separately was introduced and the resulting mixture was stirred at room temperature overnight. Then, it was washed successively with 10% aqueous citric acid (25 mL), saturated aqueous NaHCO₃ (2 × 25 mL), and brine (25 mL). The organic phase was dried (MgSO₄), evaporated under vacuum, and the

orange residue was purified by column chromatography over silica gel using dichloromethane/methanol (10:1, v/v) as the eluent. A single orange band was collected and evaporated to afford analytically pure (*S*)-**5** as an orange solid (262 mg, 97%).

^1H NMR NMR (CDCl_3): δ 0.96 (d, $^3J_{\text{HH}} = 6.4$ Hz, 3 H, CHMe_2), 0.97 (d, $^3J_{\text{HH}} = 6.4$ Hz, 3 H, CHMe_2), 1.59–1.79 (m, 3 H, CH_2CHMe_2), 3.72 (s, 3 H, OMe), 4.08 (dq, $J = 1.2, 3.1$ Hz, 1 H, fc), 4.21 (dt, $J = 1.3, 2.4$ Hz, 1 H, fc), 4.23 (dt, $J = 1.2, 2.4$ Hz, 1 H, fc), 4.26 (dq, $J = 1.2, 3.4$ Hz, 1 H, fc), 4.43 (dt, $J = 1.3, 2.5$ Hz, 1 H, fc), 4.48 (dt, $J = 1.2, 2.4$ Hz, 1 H, fc), 4.53 (dt, $J = 1.3, 2.6$ Hz, 1 H, fc), 4.62 (dt, $J = 1.3, 2.5$ Hz, 1 H, fc), 4.72 (ddd, $^3J_{\text{HH}} = 5.0, 8.6, 9.1$ Hz, 1 H, NHCH), 6.16 (d, $^3J_{\text{HH}} = 8.3$ Hz, 1 H, NH), 7.29–7.40 (m, 10 H, PPh₂). $^{13}\text{C}\{^1\text{H}\}$ NMR (CDCl_3): δ 21.82 (CHMe_2), 22.95 (CHMe_2), 25.00 (CHMe_2), 41.53 (CH_2), 50.70 (NHCH), 52.25 (OMe), 69.53 (CH fc), 69.65 (d, $J_{\text{PC}} = 1$ Hz, CH fc), 71.76 (CH fc), 71.82 (d, $J_{\text{PC}} = 1$ Hz, CH fc), 72.91 (d, $J_{\text{PC}} = 4$ Hz, CH fc), 73.15 (d, $J_{\text{PC}} = 4$ Hz, CH fc), 74.13 (d, $J_{\text{PC}} = 13$ Hz, CH fc), 74.60 (d, $J_{\text{PC}} = 15$ Hz, CH fc), 76.06 (C-CONH fc), 128.29 (2 \times d, $^3J_{\text{PC}} = 7$ Hz, CH PPh₂), 128.78 (CH PPh₂), 128.84 (CH PPh₂), 133.35 (d, $^2J_{\text{PC}} = 9$ Hz, CH PPh₂), 133.54 (d, $^2J_{\text{PC}} = 10$ Hz, CH PPh₂), 137.96 (d, $^1J_{\text{PC}} = 8$ Hz, C_{ipso} PPh₂), 138.21 (d, $^1J_{\text{PC}} = 8$ Hz, C_{ipso} PPh₂), 169.86 (CONH), 173.69 (CO_2Me). The signal due to C-P of fc was not found. $^{31}\text{P}\{^1\text{H}\}$ NMR (CDCl_3): δ -16.9 (s). IR (Nujol): ν_{NH} 3287 m, ν_{CO} 1731 vs, amide I 1622 vs, amide II 1539 vs; 1435 s, 1301 m, 1251 w, 1181 w, 1163 w, 1096 w, 1027 m, 997 w, 837 m, 744 s, 697 s, 497 m, 454 w cm^{-1} . HR MS (ESI+) calc. for $\text{C}_{30}\text{H}_{33}\text{NO}_3\text{PFe} [\text{M} + \text{H}]^+$ 542.1547, found 542.1542. $[\alpha_{\text{D}}]^{25\text{ }^\circ\text{C}} +2$ (c 0.5, CHCl_3).

***N*-(1*S*,2*S*)-1-methoxycarbonyl-2-methylbutyl] [1'-(diphenylphosphino)ferrocene-1-carboxamide] ((*S,S*)-**6**). Amide (*S,S*)-**6** was prepared similarly to (*S*)-**5**, starting with Hdpf (207 mg, 0.50 mmol), 1-hydroxybenzotriazole (81 mg, 0.60 mmol), 1-(3-dimethylaminopropyl)-3-ethylcarbodiimide (0.1 mL, 0.6 mmol), (*S,S*)-[H₃NCH(CHMeCH₂Me)CO₂Me]Cl (127 mg, 0.7 mmol) and triethylamine (0.1 mL, 0.8 mmol). Isolation as described above afforded (*S,S*)-**6** as an orange oil (255 mg, 94%).**

^1H NMR NMR (CDCl_3): δ 0.95 (t, $^3J_{\text{HH}} = 7.4$ Hz, 3 H, CH_2Me), 0.96 (d, $^3J_{\text{HH}} = 6.8$ Hz, 3 H, CHMe), 1.25 (m, 1 H, CH_2), 1.50 (m, 1H, CH_2), 1.96 (m, 1 H, CHMe), 3.72 (s, 3 H, OMe), 4.10 (dq, $J = 1.1, 3.0$ Hz, 1 H, fc), 4.22 (m, 3 H, fc), 4.42 (dt, $J = 1.2, 2.4$ Hz, 1 H, fc), 4.47 (dt, $J = 1.2, 2.4$ Hz, 1 H, fc), 4.54 (dt, $J = 1.5, 2.5$ Hz, 1 H, fc), 4.60 (dt, $J = 1.3, 2.4$ Hz, 1 H, fc), 4.69 (dd, $^3J_{\text{HH}} = 5.0, 8.7$ Hz, 1 H, NHCH), 6.16 (d, $^3J_{\text{HH}} = 8.7$ Hz, 1 H, NH), 7.28–7.40 (m, 10 H, PPh₂). $^{13}\text{C}\{^1\text{H}\}$ NMR (CDCl_3): δ 11.60 (CH_2Me), 15.74 (CHMe), 25.36 (CH_2), 37.87 (CHMe), 52.08 (OMe), 56.38 (NHCH), 69.30 (CH fc), 69.65 (d, $J_{\text{PC}} = 1$ Hz, CH fc), 71.79 (CH fc), 71.83 (d, $J_{\text{PC}} = 1$ Hz, CH fc), 72.93 (d, $J_{\text{PC}} = 4$ Hz, CH fc), 73.09 (d, $J_{\text{PC}} = 4$ Hz, CH fc), 74.15 (d, $J_{\text{PC}} = 13$ Hz, CH fc), 74.41 (d, $J_{\text{PC}} = 15$ Hz, CH fc), 76.24 (C-CONH fc), 128.24 (2 \times d, $^3J_{\text{PC}} = 7$ Hz, CH PPh₂), 128.66 (CH PPh₂), 128.72 (CH PPh₂), 133.35 (d, $^2J_{\text{PC}} = 6$ Hz, CH PPh₂), 133.54 (d, $^2J_{\text{PC}} = 7$ Hz, CH PPh₂), 138.36 (d, $^1J_{\text{PC}} = 9$ Hz, C_{ipso} PPh₂), 138.52 (d, $^1J_{\text{PC}} = 10$ Hz, C_{ipso} PPh₂), 169.84 (CONH), 172.71 (CO_2Me). The signal due to C-P of fc was not found. $^{31}\text{P}\{^1\text{H}\}$ NMR (CDCl_3): δ -17.0 (s). IR (neat): ν_{NH} 3334 m, ν_{CO} 1743 vs, amide I 1652 vs, amide II 1520 vs; 1435 s, 1299 m, 1201 w, 1179 m, 1163 s, 1094 w, 1027 m, 998 w, 833 m, 746 s, 699 s, 497 s, 451 w cm^{-1} . HR MS (ESI+) calc. for $\text{C}_{30}\text{H}_{33}\text{NO}_3\text{PFe} [\text{M} + \text{H}]^+$ 542.1547, found 542.1541. $[\alpha_{\text{D}}]^{25\text{ }^\circ\text{C}} -2$ (c 0.5, CHCl_3).

Asymmetric allylic alkylation. General procedure. Ligand (12.5 μmol), $[\text{Pd}(\mu\text{-Cl})(\eta^3\text{-C}_3\text{H}_5)_2]$ (2.3 mg, 6.3 μmol) and alkali metal acetate (25 μmol ; if appropriate) were mixed with dry dichloromethane (3 mL) and the mixture was stirred at room temperature for 20 min. Allylic substrate (0.25 mmol; 63.1 mg of acetate **11a** or 70.6 mg of carbonate ester (0.75 mmol; 0.09 mL of dimethyl malonate or 0.17 mL of di-*tert*-butyl malonate) and *N,O*-bis(trimethylsilyl)acetamide (BSA; 0.75 mmol, 0.19 mL) were introduced successively. The resulting mixture was stirred for 24 h at reaction temperature (see Table 1), and then diluted with dichloromethane (3 mL) and washed with saturated aqueous NH_4Cl (2 \times 5 mL). The organic layer was separated, dried over MgSO_4 , and evaporated under vacuum. Subsequent purification by column chromatography (silica gel; hexane-ethyl acetate, 3:1 v/v) afforded the alkylation product **12** (or its mixture with **11a** in the case of incomplete conversions).

Conversions were determined by ^1H NMR spectroscopy. Enantiomeric excesses were established from ^1H NMR spectra recorded in C_6D_6 in the presence of the chiral lanthanide shift reagent tris(3-trifluoroacetyl-*d*-camphorato)europium(III). The configuration of the major component was assigned on the basis of optical rotation.³⁴

Asymmetric allylic amination. General procedure. Ligand (*S*)-**2** (6.2 mg, 12.5 μmol) and $[\text{Pd}(\mu\text{-Cl})(\eta^3\text{-C}_3\text{H}_5)_2]$ (2.3 mg, 6.3 μmol) were mixed with dry dichloromethane (3 mL) and the mixture was stirred at room temperature for 20 min. Acetate **11a** (0.25 mmol, 63.1 mg) was introduced and, after stirring for another 5 min, benzylamine (0.75 mmol, 0.08 mL) and *N,O*-bis(trimethylsilyl)acetamide (BSA; 0.75 mmol, 0.19 mL) were added successively. The resulting mixture was stirred for 24 h or 48 h at room temperature, diluted with diethyl ether (5 mL) and washed with saturated aqueous NH_4Cl (2 \times 5 mL). The organic layer was separated, dried over MgSO_4 , and concentrated under vacuum. Subsequent purification by column chromatography (silica gel; hexane-ethyl acetate, 3:1 v/v) afforded the alkylation product (or its mixture with **11a** in the case of incomplete conversions).

Conversions were determined by ^1H NMR spectroscopy. Enantiomeric excesses were established by HPLC analysis using Daicel Chiralcel OD-H column and hexane/2-propanol 99:1 (v/v) as the eluent; $t_{\text{R}}((R)\text{-13}) = 18.4$, $t_{\text{R}}((S)\text{-13}) = 19.8$ min at a flow rate of 0.50 mL min^{-1} . The configuration was assigned on the basis of optical rotation. Spectroscopic data of the product were in accordance with the literature.³⁵

Asymmetric allylic etherification. General procedure. Ligand (*S*)-**2** (6.2 mg, 12.5 μmol) and $[\text{Pd}(\mu\text{-Cl})(\eta^3\text{-C}_3\text{H}_5)_2]$ (2.3 mg, 6.3 μmol) were mixed with dry dichloromethane (3 mL) and the mixture was stirred for 20 min. Then, acetate **11a** (0.25 mmol, 63.1 mg) was added and, after stirring for another 5 min, neat benzyl alcohol (0.75 mmol, 0.08 mL) and a base (0.75 mmol; 0.19 mL of *N,O*-bis(trimethylsilyl)acetamide or 244 mg of Cs_2CO_3) were added successively. The resulting mixture was stirred at room temperature for 24 h or 48 h, diluted with diethyl ether (5 mL) and washed with saturated aqueous NH_4Cl (2 \times 5 mL). The organic layer was separated, dried over MgSO_4 , and evaporated under reduced pressure. Purification by column chromatography (conditions as above) recovered only **11a**.

Preparation of palladium(II) complexes

[Pd(MeCN)₂(η³-C₃H₄Me)]ClO₄ (15). A solution of AgClO₄ (415 mg, 2.0 mmol) in acetonitrile (5 mL) was added to a dichloromethane solution of **14** (394 mg, 1.0 mmol in 10 mL). An off-white precipitate formed immediately and the yellow colour due to the starting Pd complex disappeared. The mixture was stirred for 10 min in the dark and filtered. The colourless filtrate was evaporated to an oil, which was taken up with acetonitrile (5 mL). The solution was precipitated with diethyl ether (35 mL), yielding an oil, which quickly crystallised. The separated product was filtered off, washed with diethyl ether and dried under vacuum. Yield: 542 mg (79%), white powdery solid. Note: The product is quite stable in the air but deposits Pd(0) upon prolonged standing. It appropriate, it can be purified by dissolving in acetonitrile, filtration and precipitation with diethyl ether.

¹H NMR (CDCl₃): δ 2.16 (s, 3 H, Me allyl), 2.41 (s, 6 H, MeCN), 3.04 and 4.41 (2× br s, 2 H, CH₂ allyl). ¹³C{¹H} NMR (CDCl₃): δ 3.13 (MeCN), 22.81 (Me allyl), 63.04 (CH₂ allyl), 121.92 (MeCN), 134.41 (C_{ipso} allyl). IR (Nujol): 2318 m, 2292 m, ν₃(ClO₄) 1098/1082 vs composite, ν₁(ClO₄) 931 w, 961 m, 839 m, ν₄(ClO₄) 624 s cm⁻¹. Anal. calc. for C₈H₁₃ClNO₄Pd: C 28.01, H 3.82, N 8.17%. Found: C 28.23, H 3.95, N 8.24%.

[(η³-C₃H₄Me)PdCl(1-κP)] (16). A solution of **1** (146 mg, 0.30 mmol) in chloroform (3 mL) was added to solid [Pd(μ-Cl)(η³-C₃H₄Me)₂] (**14**; 59 mg, 0.15 mmol). The reaction mixture was stirred at room temperature for 1 h and then poured into pentane (30 mL). After standing at -18 °C overnight, the precipitated product was filtered off, washed thoroughly with pentane and dried under vacuum. Yield: 195 mg (95%), yellow solid.

¹H NMR NMR (CDCl₃): δ 1.89 (s, 3 H, Me allyl), 2.47 (s, 1 H, CH₂ allyl), 2.81 (s, 1 H, CH₂ allyl), 3.51 (d, ²J_{HH} = 10 Hz, 1 H, CH₂ allyl), 4.29 (m, 1 H, C-C₅H₄), 3.72 (s, 3 H, OMe), 3.90 (m, 1 H, C-C₅H₄), 3.94 (dd, ²J_{HH} = 17.5 Hz, ³J_{HH} = 5.8 Hz, 1 H, CH₂NH), 4.21 (dd, ²J_{HH} = 17.5 Hz, ³J_{HH} = 6.4 Hz, 1 H, CH₂NH), 4.29 (m, 1 H, P-C₅H₄), 4.44 (dd, ²J_{HH} = 6.8 Hz, ³J_{PH} = 3.0 Hz, 1 H, CH₂ allyl), 4.61 (m, 1 H, P-C₅H₄), 4.70 (m, 1 H, P-C₅H₄), 4.81 (m, 1 H, P-C₅H₄), 5.02 (m, 1 H, C-C₅H₄), 5.31 (m, 1 H, C-C₅H₄), 7.31–7.54 (m, 8 H, PPh₂), 7.79–7.86 (m, 2 H, PPh₂), 7.92 (t, ³J_{HH} = 5.9 Hz, 1 H, NH). ¹³C{¹H} NMR (CDCl₃): δ 23.12 (Me allyl), 41.05 (CH₂N), 51.96 (OMe), 64.13 (CH₂ allyl), 70.07 (CH C-C₅H₄), 70.32 (CH C-C₅H₄), 71.94 (2C, CH C-C₅H₄), 73.37 (d, J_{PC} = 10 Hz, CH P-C₅H₄), 73.55 (d, J_{PC} = 6 Hz, CH P-C₅H₄), 74.25 (d, J_{PC} = 46 Hz, C_{ipso} P-C₅H₄), 74.41 (d, J_{PC} = 9 Hz, CH P-C₅H₄), 76.90 (C_{ipso} C-C₅H₄), 78.65 (d, ²J_{PC} = 32 Hz, CH₂ allyl), 128.29 (d, ³J_{PC} = 10 Hz, CH_{meta} PPh₂, 4C), 129.77 (d, ⁴J_{PC} = 1 Hz, CH_{para} PPh₂), 130.26 (d, ⁴J_{PC} = 2 Hz, CH_{para} PPh₂), 132.27 (d, ²J_{PC} = 12 Hz, CH_{ortho} PPh₂), 133.37 (d, ²J_{PC} = 5 Hz, C_{ipso} allyl), 133.69 (d, ²J_{PC} = 12 Hz, CH_{ortho} PPh₂), 135.06 (d, ¹J_{PC} = 43 Hz, C_{ipso} PPh₂), 137.56 (d, ¹J_{PC} = 44 Hz, C_{ipso} PPh₂), 170.05 (CONH), 170.82 (CO₂Me). A resonance due to one CH of P-C₅H₄ is obscured by the solvent signal. ³¹P{¹H} NMR (CDCl₃): δ 11.6 (s). IR (Nujol): ν_{NH} 3305 m, ν_{CO} 1750 vs, amide I 1652 vs, amide II 1538 vs, 1436 vs, 1304 m, 1211 s, 1196 s, 1178 s, 1098 m, 1172 w, 1030 m, 979 w, 837 m, 750 s, 697 vs, 629 w, 617 w, 519 m, 497 w, 471 w cm⁻¹. ESI MS: m/z 646 ([M - Cl]⁺). Anal. calc. for C₃₀H₃₁ClFeNO₃PPd·0.15 CH₂Cl₂: C 52.10, H 4.54, N 2.02%. Found: C 52.19, H 4.54, N 1.79%. The amount of solvent was confirmed by NMR.

[(η³-C₃H₄Me)Pd(1-κ²O,P)]ClO₄ (17). A solution of **1** (43 mg, 0.09 mmol) in chloroform (2 mL) was added to solid [Pd(MeCN)₂(η³-C₃H₄Me)]ClO₄ (**15**; 30 mg, 0.09 mmol). The resulting mixture was stirred at room temperature for 1 h and then poured into pentane (30 mL). After standing overnight at -18 °C, the precipitated product was filtered off, washed with pentane and dried under vacuum. Yield: 63 mg (96%), yellow solid.

¹H NMR NMR (CDCl₃): δ 2.18 (s, 3 H, Me allyl), 2.94 (br d, ³J_{HH} = 2.0 Hz, 1 H, CH₂ allyl), 3.10 (br q, ³J_{HH} ≈ 2.6 Hz, 1 H, CH₂ allyl), 3.68 (s, 3 H, OMe), 4.06 (d, ²J_{HH} = 9.3 Hz, 1 H, CH₂ allyl), 4.08 (br m, 1 H, P-C₅H₄), 4.16 (d, ³J_{HH} = 6.0 Hz, 2 H, CH₂NH), 4.29 (br m, 1 H, P-C₅H₄), 4.39 (br dt, ³J_{HH} = 1.3, 2.6 Hz, 1 H, C-C₅H₄), 4.44 (br dt, ³J_{HH} = 1.3, 2.6 Hz, 1 H, C-C₅H₄), 4.64 (br m, 1 H, P-C₅H₄), 4.71–4.76 (br m, 2 H, CH₂ allyl + P-C₅H₄), 5.16 (br dt, ³J_{HH} = 1.3, 2.6 Hz, 1 H, C-C₅H₄), 5.32 (br dt, ³J_{HH} = 1.3, 2.6 Hz, 1 H, C-C₅H₄), 7.41–7.54 (m, 10 H, PPh₂), 8.07 (t, ³J_{HH} = 5.9 Hz, 1 H, NH). ¹³C{¹H} NMR (CDCl₃): δ 23.23 (Me allyl), 42.04 (CH₂N), 52.16 (OMe), 55.44 (CH₂ allyl), 71.56 (d, J_{PC} = 49 Hz, C_{ipso} P-C₅H₄), 71.73 (CH C-C₅H₄), 71.96 (CH C-C₅H₄), 72.71 (CH C-C₅H₄), 72.96 (CH C-C₅H₄), 73.85 (d, J_{PC} = 7 Hz, CH P-C₅H₄), 74.27 (d, J_{PC} = 7 Hz, CH P-C₅H₄), 74.35 (C_{ipso} C-C₅H₄), 75.00 (d, J_{PC} = 10 Hz, CH P-C₅H₄), 75.76 (d, J_{PC} = 12 Hz, CH P-C₅H₄), 83.34 (d, ²J_{PC} = 27 Hz, CH₂ allyl), 129.01 (d, ³J_{PC} = 10 Hz, CH_{meta} PPh₂), 129.07 (d, ³J_{PC} = 10 Hz, CH_{meta} PPh₂), 131.19 (d, ⁴J_{PC} = 2 Hz, CH_{para} PPh₂), 131.29 (d, ⁴J_{PC} = 2 Hz, CH_{para} PPh₂), 132.00 (d, ¹J_{PC} = 45 Hz, C_{ipso} PPh₂), 132.77 (d, ²J_{PC} = 13 Hz, CH_{ortho} PPh₂), 133.01 (d, ²J_{PC} = 14 Hz, CH_{ortho} PPh₂), 136.09 (d, ²J_{PC} = 5 Hz, C_{ipso} allyl), 169.51 (CO₂Me), 174.12 (CONH). ³¹P{¹H} NMR (CDCl₃): δ 20.8 (s). IR (Nujol): ν_{NH} 3350 m, ν_{CO} 1754 vs, 1652 m, amide I 1596 vs, amide II 1558 vs, 1436 vs, 1311 m, 1213 s, 1198 s, 1169 s, ν₃(ClO₄) 1097 br vs, ν₁(ClO₄) 930 w, 908 w, 837 m, 750 s, 697 vs, ν₄(ClO₄) 624 vs, 471 vs. cm⁻¹. ESI MS: m/z 646 ([M - ClO₄]⁺; i.e., the cation). Anal. calc. for C₃₀H₃₁ClFeNO₇PPd·0.25C₅H₁₂: C 49.27, H 4.53, N 1.82%. Found: C 49.27, H 4.68, N 2.02%. The amount of solvent was verified by NMR.

[(η³-C₃H₄Me)Pd(1-κP₂)]ClO₄ (18) was prepared and isolated similarly to **17**, using **14** (34 mg, 0.10 mmol) and **1** (97 mg, 0.20 mmol). Yield: 119 mg (97%), yellow powder.

¹H NMR NMR (CDCl₃): δ 1.84 (s, 3 H, Me allyl), 3.47 (m, 2 H, CH₂ allyl), 3.69 (dt, ³J_{HH} = 1.3, 2.6 Hz, 2 H, C-C₅H₄), 3.73 (s, 8 H, OMe and CH₂ allyl), 3.78 (dt, ³J_{HH} = 1.3, 2.6 Hz, 2 H, C-C₅H₄), 4.09–4.13 (m, 6 H, CH₂NH and P-C₅H₄), 4.19 (br s, 2 H, P-C₅H₄), 4.61 (m, 2 H, P-C₅H₄), 4.63 (dt, ³J_{HH} = 1.2, 2.6 Hz, 2 H, P-C₅H₄), 4.64 (m, 2 H, C-C₅H₄), 4.68 (dt, ³J_{HH} = 1.3, 2.6 Hz, 2 H, C-C₅H₄), 7.04 (t, ³J_{HH} = 5.9 Hz, 2 H, NH), 7.24–7.51 (m, 20 H, PPh₂). ¹³C{¹H} NMR (CDCl₃): δ 23.48 (Me allyl), 41.25 (CH₂NH), 52.12 (OMe), 69.66 (CH C-C₅H₄), 69.95 (CH C-C₅H₄), 72.13 (CH C-C₅H₄), 72.36 (CH C-C₅H₄), 73.69 (t, J' = 6 Hz, CH P-C₅H₄), 73.93 (t, J' = 4 Hz, CH P-C₅H₄), 74.08 (t, J' = 4 Hz, CH P-C₅H₄), 74.58 (t, J' = 7 Hz, CH P-C₅H₄), ca. 76.6 (CH₂ allyl; partly obscured by the solvent signal), 78.25 (t, J' = 23 Hz, C_{ipso} P-C₅H₄), 128.70 (t, J' = 5 Hz, CH_{meta} PPh₂), 128.78 (t, J' = 5 Hz, CH_{meta} PPh₂), 130.94 (CH_{para} PPh₂), 131.29 (CH_{para} PPh₂), 131.40 (d, J' = 23 Hz, C_{ipso} PPh₂), 132.08 (d, J' = 23 Hz, C_{ipso} PPh₂), 132.85 (t, J' = 6 Hz, CH_{ortho} PPh₂), 133.20 (t, J' = 7 Hz, CH PPh₂), 137.70 (t, J' = 5 Hz, C_{ipso} allyl), 169.68 (CONH), 170.59 (CO₂Me). The resonance due to C_{ipso} of C-C₅H₄ overlaps with the signal of solvent. ³¹P{¹H} NMR (CDCl₃): δ 18.2 (s). IR

Table 5 Summary of crystallographic parameters, data collection and structure refinement parameters for **15**, **16**·H₂O and **17**^a

Compound	15	16 ·H ₂ O	17
Formula	C ₈ H ₁₃ ClN ₂ O ₄ Pd	C ₃₀ H ₃₃ ClFeNO ₄ PPd	C ₃₀ H ₃₁ ClFeNO ₄ PPd
<i>M</i>	343.05	700.24	746.23
Crystal system	Monoclinic	Monoclinic	Monoclinic
Space group	<i>P</i> 2 ₁ / <i>m</i> (no. 14)	<i>P</i> 2 ₁ / <i>c</i> (no. 14)	<i>P</i> 2 ₁ / <i>n</i> (no. 14)
<i>a</i> /Å	7.3756(2)	10.0468(7)	14.4397(6)
<i>b</i> /Å	10.4597(3)	30.550(2)	15.1067(6)
<i>c</i> /Å	8.3592(2)	9.7502(7)	15.0910(7)
β (°)	95.8421(17)	105.252(4)	112.494(1)
<i>U</i> /Å ³	641.53(3)	2887.2(3)	3041.4(2)
<i>Z</i>	2	4	4
μ (Mo-K α)/mm ⁻¹	1.655	1.310	1.256
<i>T</i> ^b	0.654–0.750	0.603–0.711	0.641–0.746
Diffns collected	8315	28502	26854
Unique diffns	1543	6639	6962
Obsd ^c diffns	1505	5960	4760
<i>R</i> _{int} ^d /%	2.78	2.65	3.96
<i>R</i> ^d obsd diffns/%	1.76	3.22	3.86
<i>R</i> , <i>wR</i> ^d all data/%	1.80, 4.45	3.77, 7.47	7.69, 10.3
$\Delta\rho$ /e Å ⁻³	0.41, -0.46	0.54 -0.46	2.02, -1.15
CCDC entry	823874	823875	823876

^a Common details: *T* = 150(2)K. ^b The range of transmission factors. ^c Observed diffractions with *I* > 2 σ (*I*). ^d $R_{\text{int}} = \sum |F_o^2 - F_c^2(\text{mean})| / \sum F_o^2$, where $F_c^2(\text{mean})$ is the average intensity of symmetry-equivalent diffractions. $R = \sum \|F_o| - |F_c|\| / \sum |F_o|$, $wR = [\sum \{(wF_o^2 - F_c^2)^2\} / \sum (wF_o^2)^2]^{1/2}$. ^e Residual electron density in vicinity of the Pd atom.

(Nujol): ν_{NH} 3385 m, ν_{CO} 1753 vs, amide I 1655 vs, amide II 1536 vs, 1437 vs, 1303 m, 1211 s, 1196 s, 1177 s, 1164 m, 1101 vs, 1037 m, 1000 w, 839 w, 748 m, 697 s, 624 m, 484 s cm⁻¹. MS (ESI⁺): *m/z* 1131 [(C₃H₄Me)Pd(1)₂]⁺, 938, 646 [(C₃H₄Me)Pd(1)]⁺. Anal. calc. for C₅₆H₅₅ClFe₂N₂O₁₀P₂Pd·0.15C₅H₁₂: C 54.86, H 4.61, N 2.26%. Found: C 54.87, H 4.90, N 2.00%. The presence of solvent was verified by NMR.

X-Ray crystallography

Single crystals suitable for X-ray diffraction analysis were grown by liquid-phase diffusion from dichloromethane-hexane (**15**: colourless block, 0.18 × 0.25 × 0.35 mm³), toluene-hexane (**16**·H₂O: orange prism, 0.28 × 0.34 × 0.43 mm³) and ethyl acetate-hexane (**17**: orange bar, 0.21 × 0.24 × 0.29 mm³).

Full-set diffraction data ($\pm h \pm k \pm l$, $2\theta_{\text{max}} = 55^\circ$, completeness $\geq 98.7\%$) were collected with a Buker Apex2 (**16**·H₂O, **17**) or a Nonius KappaCCD (**15**) diffractometers equipped with Oxford Cryosystem cooling device. The measurements were performed at 150(2) K using with graphite-monochromated Mo-K α radiation ($\lambda = 0.71073$ Å) and the data were corrected for absorption. Further details are presented in Table 5.

The structures were solved by direct methods (SHELXS-97³⁶ or SIR-97³⁷) and refined by full-matrix least-squares based on *F*² (SHELXL97³⁸). All non-hydrogen atoms were refined with anisotropic displacement parameters. The amide (NH) hydrogen in **17** and allylic hydrogens in **15** were located on difference electron density maps and refined as riding atoms. All other hydrogen atoms were included in their calculated positions and refined as riding atoms. The PdCl(η^3 -MeC₃H₄) moiety in the structure of **16**·H₂O appears to be disordered over two positions. However, because of the low contribution of the less populated orientation and overlaps, only the Pd atom could be refined over two positions (the refined occupancies were *ca.* 96.6 : 3.4). All geometric calculations were performed with a recent version of PLATON^{39,40} program.

Acknowledgements

This work was supported by the Grant Agency of Charles University in Prague (project no. 58009) and by the Ministry of Education of the Czech Republic (project nos. LC06070 and MSM0021620857).

References

- (a) G. Consiglio and R. M. Waymouth, *Chem. Rev.*, 1989, **89**, 257; (b) B. M. Trost and D. L. Van Vranken, *Chem. Rev.*, 1996, **96**, 395; (c) B. M. Trost and M. L. Crawley, *Chem. Rev.*, 2003, **103**, 2921; (d) T. Graening and H.-G. Schmalz, *Angew. Chem., Int. Ed.*, 2003, **42**, 2580; (e) B. M. Trost, *J. Org. Chem.*, 2004, **69**, 5813; (f) B. M. Trost, T. Zhang and J. D. Sieber, *Chem. Sci.*, 2010, **1**, 427; (g) T. Hayashi in *Catalytic Asymmetric Synthesis* (Ed.: I. Ojima), chapter 7.1, pp. 325-365, VCH, New York 1993; (h) I. G. Rios, A. Rosas-Hernandez and E. Martin, *Molecules*, 2011, **16**, 970.
- B. M. Trost, M. R. Machacek and A. Aponick, *Acc. Chem. Res.*, 2006, **39**, 747.
- (a) T. Hayashi in *Ferrocenes: Homogeneous Catalysis, Organic Synthesis, Materials Science* (Ed.: A. Togni and T. Hayashi), chapter 2, pp. 105-142, VCH, Weinheim, 1995; (b) H.-U. Blaser, W. Chen, F. Camponovo and A. Togni in *Ferrocenes: Ligands, Materials and Biomolecules* (Ed. P. Štěpnička), chapter 6, pp. 205-235, Wiley, Chichester 2008; (c) P. Štěpnička and M. Lamač in *Ferrocenes: Ligands, Materials and Biomolecules* (Ed. P. Štěpnička), chapter 7, pp. 237-277, Wiley, Chichester 2008; (d) C. J. Richards and A. J. Locke, *Tetrahedron: Asymmetry*, 1998, **9**, 2377; (e) T. J. Colacot, *Chem. Rev.*, 2003, **103**, 3101; (f) O. B. Sutcliffe and M. R. Bryce, *Tetrahedron: Asymmetry*, 2003, **14**, 2297; (g) L.-X. Dai, T. Tu, S.-L. You, W.-P. Deng and X.-L. Hou, *Acc. Chem. Res.*, 2003, **36**, 659; (h) R. C. J. Atkinson, V. C. Gibson and N. J. Long, *Chem. Soc. Rev.*, 2004, **33**, 313; (i) X. L. Hou, S. L. You, T. Tu, W. P. Deng, X. W. Wu, M. Li, K. Yuan, T. Z. Zhang and L. X. Dai, *Top. Catal.*, 2005, **35**, 87; (j) S. P. Flanagan and P. J. Guiry, *J. Organomet. Chem.*, 2006, **691**, 2125.
- B. M. Trost, B. Breit, S. Peukert, J. Zambrano and J. W. Ziller, *Angew. Chem., Int. Ed. Engl.*, 1995, **34**, 2386.
- (a) P. Štěpnička, J. Schulz, I. Čiřáňová and K. Fejfarová, *Collect. Czech. Chem. Commun.*, 2007, **72**, 453; (b) J. Kühnert, M. Dušek, J. Demel, H. Lang and P. Štěpnička, *Dalton Trans.*, 2007, 2802; (c) J. Kühnert, M.

- Lamač, J. Demel, A. Nicolai, H. Lang and P. Štěpnička, *J. Mol. Catal. A: Chem.*, 2008, **285**, 41; (d) J. Schulz, I. Císařová and P. Štěpnička, *J. Organomet. Chem.*, 2009, **694**, 2519; (e) P. Štěpnička, M. Krupa, M. Lamač and I. Císařová, *J. Organomet. Chem.*, 2009, **694**, 2987.
- 6 (a) M. Lamač, I. Císařová and P. Štěpnička, *Eur. J. Inorg. Chem.*, 2007, 2274; (b) M. Lamač, J. Tauchman, I. Císařová and P. Štěpnička, *Organometallics*, 2007, **26**, 5042; (c) M. Lamač, I. Císařová and P. Štěpnička, *New J. Chem.*, 2009, **33**, 1549; (d) M. Lamač, J. Tauchman, S. Dietrich, I. Císařová, H. Lang and P. Štěpnička, *Appl. Organomet. Chem.*, 2010, **24**, 326.
- 7 (a) J. Tauchman, I. Císařová and P. Štěpnička, *Organometallics*, 2009, **28**, 3288; (b) J. Tauchman, I. Císařová and P. Štěpnička, *Eur. J. Org. Chem.*, 2010, 4276.
- 8 For a review, see: P. J. Deuss, R. den Heeten, W. Laan and P. C. J. Kamer, *Chem.–Eur. J.*, 2011, **17**, 4680.
- 9 (a) B. M. Trost and D. J. Murphy, *Organometallics*, 1985, **4**, 1143; (b) M. T. El Gihani and H. Heaney, *Synthesis*, 1998, 357.
- 10 Similarly to reactions with **1**, the bridge cleavage reaction of $[(\eta^3\text{-allyl})\text{PdCl}]_2$ afforded $[(\eta^3\text{-allyl})\text{PdCl}\{\text{S-2}\}]$. However, in further reactions, this complex yielded only a material showing extremely broad NMR signals (reaction with 1 equiv. of AgClO_4), or a complex reaction mixture (reaction with 4 equiv. BSA).
- 11 $[(\eta^3\text{-allyl})\text{PdCl}(\text{1})]$: A solution of **1** (0.03 mmol) in chloroform (2 mL) was added to solid $[(\eta^3\text{-allyl})\text{PdCl}]_2$ (0.015 mmol). After stirring for 45 min, the resulting yellow-orange solution was filtered and evaporated under vacuum. $[(\eta^3\text{-allyl})\text{Pd}(\text{1})\text{ClO}_4]$: To a solution of $[(\eta^3\text{-allyl})\text{PdCl}(\text{1})]$ prepared as described above was added AgClO_4 (0.03 mmol) dissolved in dry MeCN (0.5 mL) and the mixture was stirred in the dark for 10 min. The AgCl formed was filtered off and the filtrate was evaporated to dryness yielding the product as an orange-brown solid.
- 12 Selected ^1H NMR data for the major product (in CDCl_3): δ 3.92 (s, OCH_3); 3.19 and 3.99 (two partly obscured dd, 1 H each, CH_2NH), 8.09 (br unresolved t, 1 H, CH_2NH); 4.09 (m), 5.61 (dd, $J \approx 10$ and 13 Hz) and 6.37 (dd, $J \approx 11$ and 13 Hz) (3×1 H, allylic protons); 3.93 (2 H), 3.96, 4.45, 4.62, 4.83, 4.98 and 5.50 (multiplets attributed to fc protons).
- 13 For an early example, see: D. J. Mabbott, B. E. Mann and P. M. Maitlis, *J. Chem. Soc., Dalton Trans.*, 1977, 294.
- 14 (a) P. S. Pregosin and R. W. Kunz in *NMR Basic Principles and Progress*, (Ed.: P. Diehl, E. Fluck and R. Kosfeld), vol. 16, sect. E, p. 65 and references cited therein. Springer, Berlin 1979; (b) W. H. Hersch, *J. Chem. Educ.*, 1997, **74**, 1485.
- 15 (a) X = CO_2H : P. Štěpnička, J. Podlaha, R. Gyepes and M. Polášek, *J. Organomet. Chem.*, 1998, **552**, 293; (b) X = PO_3Et_2 : P. Štěpnička, I. Císařová and R. Gyepes, *Eur. J. Inorg. Chem.*, 2006, 926; (c) X = $\text{CONH}(\text{CH}_2)_n$, Py ($n = 1, 2$; Py = pyrid-2-yl): ref. 5b; (d) X = $\text{CONHCH}_2\text{CO}_2\text{Me}$: ref. 7a; (e) X = $\text{CH}=\text{CH}_2$: P. Štěpnička and I. Císařová, *Collect. Czech. Chem. Commun.*, 2006, **71**, 215; (f) X = Py or CH_2Py : P. Štěpnička, J. Schulz, T. Klemann, U. Siemeling and I. Císařová, *Organometallics*, 2010, **29**, 3187.
- 16 P. Štěpnička, *J. Organomet. Chem.*, 2008, **693**, 297.
- 17 G. A. Kukina, V. S. Sergienko, Yu. L. Gaft, I. A. Zakharova and M. A. Porai-Koshits, *Inorg. Chim. Acta*, 1980, **45**, L257.
- 18 Ch. Elschenbroich and A. Salzer, *Organometallics, A Concise Introduction*, 2nd edn, sect. 15.3, pp. 280–287, VCH, Weinheim 1992.
- 19 C–H \cdots O interactions: (1) C1–H1B \cdots O2 ‡ , C1 \cdots O2 = 3.453(2) Å, angle at H1B = 153 $^\circ$; (2) C5–H5A \cdots O2 ‡ , C5 \cdots O2 = 3.513(3) Å, angle at H5A = 175 $^\circ$; (3) C5–H5C \cdots O3 ‡ , C5 \cdots O3 = 3.395(3) Å, angle at H5C = 141 $^\circ$; i. $1-x, -y, 1-z$; ii. $-x, -y, 1-z$; iii. $1-x, -\frac{1}{2}+y, 1-z$.
- 20 J. W. Faller, C. Blankenship, B. Whitmore and S. Sena, *Inorg. Chem.*, 1985, **24**, 4483.
- 21 P. Štěpnička and I. Císařová, *Collect. Czech. Chem. Commun.*, 2006, **71**, 279.
- 22 C. P. Butts, J. Crosby, G. C. Lloyd-Jones and S. C. Stephen, *Chem. Commun.*, 1999, 1707.
- 23 As the result, the Pd \cdots Fe separation is considerably shorter in **17** (4.0226(7) Å) than in **16**· H_2O (4.5985(7) Å).
- 24 T. G. Appleton, H. C. Clark and L. E. Manzer, *Coord. Chem. Rev.*, 1973, **10**, 335.
- 25 Hydrogen bond parameter are as follows; N–H1N \cdots O4 ‡ : N \cdots O = 3.018(5) Å, angle at H1N = 175 $^\circ$; iv. $1-x, -\frac{1}{2}+y, \frac{1}{2}-z$.
- 26 (a) R. G. Pearson, *J. Am. Chem. Soc.*, 1963, **85**, 3533; (b) F. R. Hartley, *The Chemistry of Platinum and Palladium*, Applied Science, London 1973.
- 27 (a) H. Kurosawa, *J. Organomet. Chem.*, 1987, **334**, 243; (b) D. J. Cárdenas and A. M. Echavarren, *New J. Chem.*, 2004, **28**, 338.
- 28 M. Brenner and W. Huber, *Helv. Chim. Acta*, 1953, **36**, 1109.
- 29 J. Podlaha, P. Štěpnička, J. Ludvík and I. Císařová, *Organometallics*, 1996, **15**, 543.
- 30 I. D. G. Watson, S. A. Styler and A. K. Yudin, *J. Am. Chem. Soc.*, 2004, **126**, 5086.
- 31 F. Ferioli, C. Fiorelli, G. Martelli, M. Monari, D. Savoia and P. Tobaldin, *Eur. J. Org. Chem.*, 2005, 1416.
- 32 M. Toffano, J.-Y. Legros and J.-C. Fiaud, *Tetrahedron Lett.*, 1997, **38**, 77.
- 33 W. T. Dent, R. Long and A. J. Wilkinson, *J. Chem. Soc.*, 1964, 1585.
- 34 T. Hayashi, A. Yamamoto, T. Hagihara and Y. Ito, *Tetrahedron Lett.*, 1986, **27**, 191.
- 35 T. Ohta, H. Sasayama, O. Nakajima, N. Kurahashi, T. Fujii and I. Furukawa, *Tetrahedron: Asymmetry*, 2003, **14**, 537.
- 36 G. M. Sheldrick, *SHELXS-97. Program for Crystal Structure Solution from Diffraction Data*, University of Göttingen, Germany, 1997.
- 37 A. Altomare, M. C. Burla, M. Camalli, G. L.ascarano, C. Giacovazzo, A. Guagliardi, A. G. G. Moliterni, G. Polidori and R. Spagna, *J. Appl. Crystallogr.*, 1999, **32**, 115.
- 38 G. M. Sheldrick, *SHELXL-97. Program for Crystal Structure Refinement from Diffraction Data*, University of Göttingen, Germany, 1997.
- 39 A. L. Spek, *PLATON-A Multipurpose Crystallographic Tool*, Utrecht University, Utrecht, The Netherlands, 2003 and updates. For a reference, see: A. L. Spek, *J. Appl. Crystallogr.*, 2003, **36**, 7.
- 40 All numerical values are rounded with respect to their estimated standard deviations (esd's) given with one decimal. Parameters concerning atoms in fixed positions (hydrogens) are given without esd's.